Two Behavioral States Studied in a Single PET/FDG Procedure: Error Analysis

Jen Yueh Chang, Ranjan Duara, William Barker, Anthony Apicella, Fumihito Yoshii, Roger E. Kelley, Myron D. Ginsberg, and Thomas E. Boothe

Baumritter Institute of Nuclear Medicine, Mount Sinai Medical Center, Miami Beach, Florida; Departments of Radiology, and Department of Neurology, University of Miami, School of Medicine, Miami, Florida

In a previous publication the theory, procedure, and results of a method were described for making two sequential measurements of cerebral metabolic rate for glucose (CMRglc), within a 2-hr period, using [^{18}F]fluorodeoxyglucose. The error that is specific to this technique was estimated using computer simulations. CMRglc for the second state was sensitive to errors in (a) the values of the rate constants, (b) alignment of PET slices between the two scans, and (c) subtraction of one PET image from another. The root mean square of the average error from each error source was 6.4%, which gives the theoretical reliability of this method. The measured reproducibility, taken from our previous publication, was 4.2–6.2%, which is in good agreement with the present result. This method contributes a small additional error above that expected for two independent scans. However, independent scans done on different days are likely to be subject to larger physiological variations in CMRglc than would occur using this method.

J Nucl Med 30:93–105, 1989

We have previously described the theory, procedure, and results of a method for calculating, from a single extended study, two sets of regional cerebral metabolic rates of glucose (rCMRglc) values, representing two steady-state conditions (*1*). The procedure requires two injections of fluorine-18 (^{18}F) fluorodeoxyglucose (FDG), 50 min apart, and two positron emission tomography (PET) scans. From the first scan rCMRglc1 can be calculated using the tracer concentration in tissue ($C^*(T_1)$) at $T_1(T_1 = 50$ min). From the second scan rCMRglc2, the metabolic rate for the second condition, can be calculated using the tracer concentration in tissue ($C^*(T_2)$) at $T_2(T_2 = 100$ min) after subtracting out the remnant of tracer from the first injection ($R^*(T_2{:}T_1)$) to obtain $C\overset{*}{S}(T_2{:}T_1)$, which is the tracer accumulated after the second injection only. The detailed definition of the terms used in this paper are summarized in Appendix 1. To obtain the correct value of $R^*(T_2{:}T_1)$ it is necessary to know the value of each rate constant (k_2^*, k_3^*, and k_4^*) for each brain region. Since this is not available, we use average rate constant values to obtain an estimated value of $R^*(T_2{:}T_1)$, i.e., $\bar{R}^*(T_2{:}T_1)$. Consequently, error is introduced into the determination of $\bar{R}^*(T_2{:}T_1)$, which is then propagated to the estimated value of $C\overset{*}{S}(T_2{:}T_1)$, i.e., $(\overline{C\overset{*}{S}}(T_2{:}T_1))$, and to rCMRglc2. Thus, the accuracy of CMRglc2 determination is not only dependent on the accuracy of using an operational equation (*2–4*) but is also dependent on the accuracy of $\overline{C\overset{*}{S}}(T_2{:}T_1)$ determination.

A second source of error in the double injection procedure derives from difficulties in obtaining exact slice relocation for the second scan so that $\bar{R}^*(T_2{:}T_1)$ can be subtracted from the measured value of $C^*(T_2)$. In practice, however, some error in slice location is likely. These errors can be minimized by using a customized head mold (*5*) to reduce head movement and repeatedly checking head position during the procedure to assure accurate repositioning. For example, the rotational error around the z-axis in the transverse plane (Fig. 1A) and around the y-axis in the coronal plane (Fig. 1B) can be minimized with the help of a laser light, used prior to and periodically during the second PET scan. However, repositioning in the z-axis, either because of translational error (Fig. 1C) or because of rotational error around the x-axis in the sagittal plane (Fig. 1D), can only be done prior to the scan, since it is difficult to reconfirm the exact position, once the head

Received Jan. 27, 1988; revision accepted Aug. 31, 1988.

For reprints contact: Jen Yueh Chang, MS, Dept. of Neurology(D4-5), University of Miami, PO Box 016960, Miami, FL 33101.

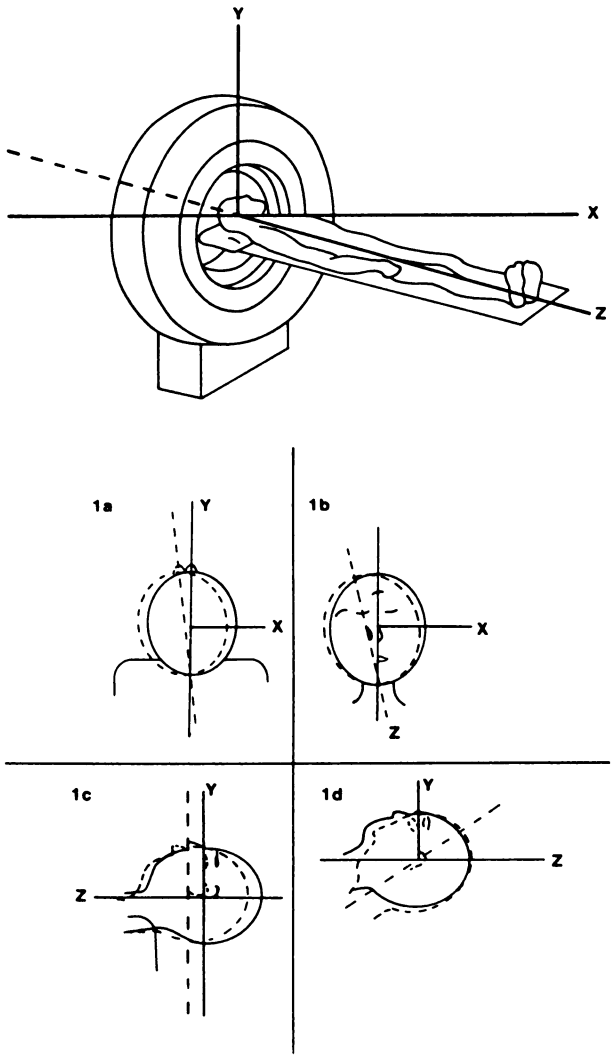

FIGURE 1
Illustration of possible sources of repositioning errors in rCMRglc2 estimation. The x-axis is defined as the axis that is parallel to the floor and normal to the long axis of the patient, the y-axis is defined as the axis that is normal to the floor, where the z-axis is defined as the axis that is parallel to the long axis of the patient's body and goes through the gantry. The most prominent repositioning errors are: (A) rotational error around the z-axis, (B) rotational error around the y-axis, (C) translational error along z-axis, and (D) rotational error around the x-axis.

is inside the scanner. Therefore, the most frequent errors are along the z-axis.

Another source of error derives from the inability to continue to maintain a specified behavioral condition during the 20-min scanning period. This poses a problem, because the desired steady-state condition gets diluted by the nonspecific scanning condition. For example, if there is less glucose metabolism in a brain structure during the scanning period relative to the activation state, by the end of the scanning period an underestimation of the glucose metabolic rate for that structure may occur due to the admixture of a period of reduced metabolism. The resulting additional error that is added to the measured rCMRglc, has been examined through computer simulations, using the example of a hypothetical instantaneous physiological change that could occur from a focal seizure (*6*) 30 min after the injection of FDG. In this paper, we draw a parallel between this example and the interruption of the steady-state due to the inability to maintain the activation state during the PET scanning period. Although this error is not specific to the double-injection method, it merits consideration here because the double injection method is likely to be used in the comparison of an activation state to a baseline state. The dilution error is probably nonexistent for the baseline state, but may be important in the activation state.

Other sources of error in rCMRglc estimation, using the deoxyglucose model with PET/FDG, have been well documented (*6,7*). The double activation/double injection method inherits these same errors as well. In this paper, the above-mentioned errors, unique to the double injection/double activation method, are addressed. Computer simulations have been used to examine the sensitivity of rCMRglc measurement to these errors. The magnitude of these errors should be assessed in terms of the errors associated with an alternative method. The utility of the double-injection method is in conveniently obtaining sequentially two sets of metabolic values. Therefore, the appropriate comparison, in terms of error analysis, would be to the situation when two independent PET/FDG scans are performed on different days in the same patient.

METHOD

rCMRglc2 is obtained by operational Eq. (1), which is an adaptation of the original operational equation proposed by Sokoloff et al. (*8*), modified by Chang et al. (*1*) as follows:

$$\text{rCMRglc2} = \frac{Cp\,\bar{k}_1^*\bar{k}_3^*}{LC[\bar{k}_2^* + \bar{k}_3^*]} \frac{\bar{C}\bar{s}^*(T_2{:}T_1)}{[\bar{C}\bar{e}^*(T_2{:}T_1) + \bar{C}\bar{m}^*(T_2{:}T_1)]}, \quad (1)$$

where Cp is the mean glucose concentration in plasma during the second behavioral state, and $\bar{k}_1^*$, $\bar{k}_2^*$, $\bar{k}_3^*$, $\bar{k}_4^*$ are average rate constant values. LC is the lumped constant (*8*), $\bar{C}\bar{s}^*(T_2{:}T_1)$ is the estimated tracer concentration that is accumulated in cerebral tissue from FDG in plasma, between times T_1 and T_2, measured by PET, and $\bar{C}\bar{e}^*(T_2{:}T_1)$ and $\bar{C}\bar{m}^*(T_2{:}T_1)$ are the estimated FDG and FDG-6-P concentrations, accumulated in cerebral tissue from FDG in plasma between T_1 and T_2. Both $\bar{C}\bar{e}^*(T_2{:}T_1)$ and $\bar{C}\bar{m}^*(T_2{:}T_1)$ are obtained analytically from the following two equations (*1*),

$$\bar{C}\bar{e}^*(T_2{:}T_1) = \frac{\bar{k}_1^*}{\bar{a}_2 - \bar{a}_1}[(\bar{k}_4^* - \bar{a}_1)e^{-\bar{a}_1(T_2-T_1)} + (\bar{a}_2 - \bar{k}_4^*)e^{-\bar{a}_2(T_2-T_1)}] \otimes \hat{C}\bar{p}^*(T_2 - T_1) \quad (2a)$$

$$\bar{C}\bar{m}^*(T_2{:}T_1) = \frac{\bar{k}_1^*\bar{k}_3^*}{\bar{a}_2 - \bar{a}_1}[e^{-\bar{a}_1(T_2-T_1)} - e^{-\bar{a}_2(T_2-T_1)}] \otimes \hat{C}\bar{p}^*(T_2 - T_1) \quad (2b)$$

where

$$\bar{a}_1 = [\bar{k}_2^* + \bar{k}_3^* + \bar{k}_4^* - \sqrt{(\bar{k}_2^* + \bar{k}_3^* + \bar{k}_4^*)^2 - 4\bar{k}_2^*\bar{k}_4^*}\,]/2$$

$$\bar{a}_2 = [\bar{k}_2^* + \bar{k}_3^* + \bar{k}_4^* + \sqrt{(\bar{k}_2^* + \bar{k}_3^* + \bar{k}_4^*)^2 - 4\bar{k}_2^*\bar{k}_4^*}\,]/2$$

and $\otimes$ denotes the operation of convolution. That is,

$$p(t) \otimes q(t) = \int_0^t p(\tau)q(t-\tau)\,d\tau\ \hat{C}p(t) = Cp(t + T_1),$$

$Cp(t)$ is the history of plasma FDG concentration from $t = 0$ onwards. $\hat{C}p(t)$ is the history of plasma FDG concentration from $t = T_1$ onwards. $\bar{C}\bar{s}^*(T_2{:}T_1)$ is obtained by subtracting $\bar{R}^*(T_2{:}T_1)$ from $C^*(T_2)$, and $\bar{R}^*(T_2{:}T_1)$ is obtained by the following equation:

$$\bar{R}^*(T_2{:}T_1) = C^*(T_1)[\bar{A}^*(T_2{:}T_1) - \bar{B}^*(T_2{:}T_1)], \qquad (3)$$

where

$$\bar{A}^*(T_2{:}T_1) = \left[\frac{\bar{a}_2}{(\bar{a}_2 - \bar{a}_1)} - \frac{\bar{k}_2^*\bar{C}\bar{e}^*(T_1)}{(\bar{a}_2 - \bar{a}_1)(\bar{C}\bar{e}^*(T_1) + \bar{C}\bar{m}^*(T_1))}\right] e^{-\bar{a}_1(T_2 - T_1)} \qquad (4a)$$

$$\bar{B}^*(T_2{:}T_1) = \left[\frac{\bar{a}_1}{(\bar{a}_2 - \bar{a}_1)} - \frac{\bar{k}_2^*\bar{C}\bar{e}^*(T_1)}{(\bar{a}_2 - \bar{a}_1)(\bar{C}\bar{e}^*(T_1) + \bar{C}\bar{m}^*(T_1))}\right] e^{-\bar{a}_2(T_2 - T_1)}. \qquad (4b)$$

Sensitivity of rCMRglc to Errors Arising from Using Average Rate Constant Values

To simplify the notations in Eq. (1), $[\bar{k}_1^*\bar{k}_3^*/(\bar{k}_2^* + \bar{k}_3^*)]/[\bar{C}\bar{e}^*(T_2{:}T_1) + \bar{C}\bar{m}^*(T_2{:}T_1)]$ is denoted as $\bar{G}(T_2{:}T_1)$, and the equation becomes as follows:

$$rCMRglc2 = \frac{Cp}{LC}\bar{G}(T_2{:}T_1)\bar{C}\bar{s}^*(T_2{:}T_1). \qquad (5)$$

By differentiating Eq. (5), taking the rate constants as independent variables, the following equation is derived:

$$d(rCMRglc2) = \sum_{i=1}^{4} \frac{Cp}{LC}\left[\bar{G}(T_2{:}T_1)\frac{\partial \bar{C}\bar{s}^*(T_2{:}T_1)}{\partial k_i^*} + \bar{C}\bar{s}^*(T_2{:}T_1)\frac{\partial \bar{G}(T_2{:}T_1)}{\partial k_i^*}\right] dk_i^* \qquad (6)$$

and

$$\frac{d(rCMRglc2)}{rCMRglc2} = \sum_{i=1}^{4}\left[\frac{k_i^*}{\bar{C}\bar{s}^*(T_2{:}T_1)}\frac{\partial \bar{C}\bar{s}^*(T_2{:}T_1)}{\partial k_i^*} + \frac{k_i^*}{\bar{G}(T_2{:}T_1)}\frac{\partial \bar{G}(T_2{:}T_1)}{\partial k_i^*}\right]\frac{dk_i^*}{k_i} \qquad (7)$$

where

$$\frac{\partial W}{\partial k_i} = \frac{W(k_i + \Delta k_i) - W(k_i)}{\Delta k_i}.$$

k_i are the rate constants ($i = 1$ to 4). Equation (7) shows that the percent error of rCMRglc2 is the sum of percent error from each rate constant multiplied by a composite term consisting of $\bar{G}(T_2{:}T_1)(\bar{C}\bar{s}^*(T_2{:}T_1))$ and the partial derivatives of $\bar{G}(T_2{:}T_1)(\bar{C}\bar{s}^*(T_2{:}T_1))$ to each rate constant. The coefficient of variation (CV) of rCMRglc2, caused by using erroneous values of rate constants, can then be estimated from Eq. (7), provided that the CV of each rate constant is known.

A synthetic three-parameter function, derived from plasma radioactivity curves and pooled from four patients, was used to simulate the arterial input function of FDG to include two injections at separate times. It is expressed mathematically as follows:

$$Ca(t) = 0.56e^{-2.98*t} + 0.26e^{-0.14*t} + 0.19e^{-0.016*t} + B[0.56e^{-2.98*(t-T_1)} + 0.26e^{-0.14*(t-T_1)} + 0.19e^{-0.016*(t-T_1)}],$$

where $B = 0$, when $t < T_1$ and $B = R$, when $t > T_1$ (R is the ratio of second injection dose to first injection dose and T_1 is the time of the second injection).

The values of true $C^*(t)$ (i.e., $C\bar{e}^*(t) + C\bar{m}^*(t)$), $R^*(t{:}T_1)$, and $C\bar{s}^*(t{:}T_1)$ at any time t can be predicted analytically, using the appropriate rate constant values and time T_1, as we have previously shown (*1*). Values for $\bar{R}^*(T_2{:}T_1)$, $\bar{C}\bar{s}^*(T_2{:}T_1)$ and $\bar{G}(T_2{:}T_1)$ can be obtained by Eqs. (2) and (3) using published average rate constant values (*2*). Error sensitivity, defined as the multiple of unit percent error of the dependent variable that is subjected to a unit percent error of the independent variable, is used here to examine how the accuracy of $\bar{C}\bar{s}^*(T_2{:}T_1)$ and rCMRglc2 measurements is affected by using erroneous rate constant values.

Sensitivity of rCMRglc Estimation Arising from Positioning Error

A simplified one-dimensional model, assuming the major positioning errors between the two PET scans would arise along the z-axis, is used to examine how the rCMRglc2 measurement is affected by positioning errors. The possible percent errors of rCMRglc2, from positioning errors, were evaluated using simulated z-axis point-spread-functions (PSF) (Fig. 2) and the following equation, derived from the simplified model (Appendix 2),

$$\frac{\Delta \bar{C}\bar{s}^*(T_2{:}T_1, Z_0)}{\bar{C}\bar{s}^*(T_2{:}T_1, Z_0)} \times 100\% = \frac{\dfrac{\Delta C^*(T_2, Z_0)}{C^*(T_2, Z_0)}}{1 - \dfrac{R^*(T_2{:}T_1, Z_0)}{C^*(T_2, Z_0)}} \times 100\% \qquad (8)$$

The equation suggests that the magnitude of error of $\bar{C}\bar{s}^*(T_2{:}T_1, Z_0)$ is dependent on how large a difference of $C^*(T_2)$ there is along the z-axis and also the magnitude of $R^*(T_2{:}T_1)$ present in $C^*(T_2)$.

To simplify the computer simulation, we assumed that rCMRglc values for both states were identical, i.e., rCMRglc1 − rCMRglc2 = 0. Therefore, any differences obtained between rCMRglc2 and rCMRglc1 would have been generated by positioning error alone. Computer simulations were performed to examine error at a hypothetical site that had an abrupt 25% change of tracer concentration (step-change) along the z-axis.

Error of rCMRglc Estimation Arising from the Ill-Defined Behavioral State During the Scanning Period

Combinations (sets) of FDG transport rate constant values (Appendix 3) that predict different metabolic rates (all other

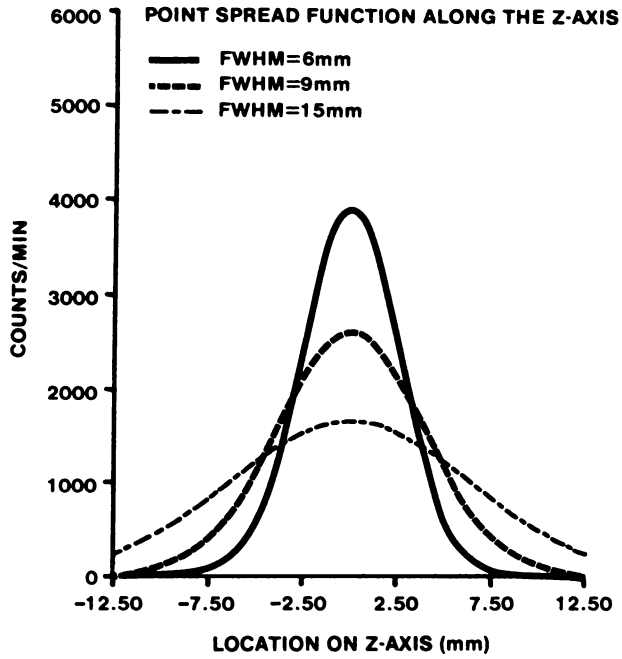

FIGURE 2
Illustration of the three point-spread functions along the z-axis that were used to examine the error of CMRglc2 due to repositioning error.

factors being constant) were used to examine the magnitude of dilution of CMRglc values, resulting from the admixture of the desired behavioral condition by the ill-defined condition during the period of scanning. Rate constants from Appendix 3 for the specific behavioral state and the resting state were used to calculate cerebral FDG accumulation during the task period and scanning period, respectively. To simplify the computer simulation, we have assumed the transition from the activation state to the resting state happened instantaneously and that the rate constant changes also occurred instantaneously. The values of the rate constants for each behavioral condition were obtained by assuming that the specific behavioral condition had a 20% higher rCMRglc value than the nonspecific scanning (resting) condition.

RESULTS

Error Sensitivity of $\overline{C}\overset{*}{s}(T_2:T_1)$ to Rate Constants

Figure 3 shows the relationship of $C\overset{*}{s}(t:T_1)$, $R^*(t:T_1)$, and $C^*(t)$ in μCi/cc from t = 50 min onwards for four different conditions, i.e., when there is no second FDG injection (injection dose ratio (IDR) = 1:0), and with a second FDG injection using, respectively, 50% (IDR = 1:0.5), 100% (IDR = 1:1), and 200% of the initial dose (IDR = 1:2). These plots and Table 1 illustrate the ratio of $\overline{C}\overset{*}{s}(T_2:T_1)/R^*(T_2:T_1)$, i.e., the ratio of the distance between the solid line and the dashed line to the distance between the dashed line and the baseline, increases as the FDG dose is increased in the second injection. Thus the accuracy of $\overline{C}\overset{*}{s}(T_2:T_1)$ measurement can be improved by increasing the dose of the second FDG injection. The error sensitivity of $\overline{C}\overset{*}{s}(T_2:T_1)$ to k_1^* remained at 0 for all cases (Fig. 4A), since the estimation of $\overline{C}\overset{*}{s}(T_2:T_1)$ is not a function of k_1^* [Eq. (4a) and (4b)]. Whereas, Fig. 4B–D shows that the error sensitivities of $\overline{C}\overset{*}{s}(T_2:T_1)$ to k_2^*, k_3^*, and k_4^* decrease as the dose of the second injection increases. These values, describing the error sensitivities of the rate constants, were all small, suggesting that the error in $\overline{C}\overset{*}{s}(T_2:T_1)$ estimation is not very sensitive to the errors in the rate constants. For example, for a 1% error of k_2^*, 0.06% and 0.034% errors of $\overline{C}\overset{*}{s}(T_2:T_1)$ were obtained for 1:1 and 1:2 injection dose ratios, respectively, when T_2 = 100 min (50 min after second FDG injection) and T_1 = 50 min. The error sensitivities to k_3^* and k_4^* are of about the same order as for k_2^*. The CV of $\overline{C}\overset{*}{s}(T_2:T_1)$ (arising from the use of erroneous rate constants) is shown in Figure 5. The values of the CV of $\overline{C}\overset{*}{s}(T_2:T_1)$ were obtained using the published average CV of each rate constant (*2*), i.e., 27.5% for k_1^*, 50.8% for k_2^*, 30.6% for k_3^*, and 17.4% for k_4^*. The CV of $\overline{C}\overset{*}{s}(T_2:T_1)$ for each injection dose ratio is maximal at 3 min after the second injection, and, then gradually declines reaching a minimum value at 65 min after the second FDG injection, after which it increases again. This minimum CV occurs because of the decreasing error sensitivities of $\overline{C}\overset{*}{s}(T_2:T_1)$ to k_2^* and k_3^*, but increasing error sensitivity of $\overline{C}\overset{*}{s}(T_2:T_1)$ to k_4^*. This minimum is ~4.0% at 65 min after the second FDG injection, for a 1:1 injection dose ratio, and about 2.3% for a 1:2 injection dose ratio.

Sensitivity of rCMRglc to Errors in Rate Constants

Figure 6 shows the error sensitivities of rCMRglc1 and rCMRglc2 to each rate constant. rCMRglc1 and rCMRglc2 values are insensitive to errors in k_1^*; the explanation for rCMRglc1 being insensitive to k_1^* errors has already been given (*4*). Insensitivity of rCMRglc2 to error in k_1^* occurs because both $\overline{G}(T_2:T_1)$ and $\overline{C}\overset{*}{s}(T_2:T_1)$ are not functions of k_1^*. Errors of k_2^* and k_3^* result in greater error in rCMRglc1 than rCMRglc2. But for error of k_4^*, the effect is reversed. The reason for this reversal is apparent from Eq. (7), which shows that the combination of error in $\overline{G}(T_2:T_1)$ (dashed line in Fig. 6) and $\overline{C}\overset{*}{s}(T_2:T_1)$ (line of IDR = 1:1 in Fig. 4) results in error cancellation for k_2^* and k_3^*, but in error summation for k_4^*. Thus, the overall CV of rCMRglc2, using a 1:1 injection dose ratio, reaches its minimum (4.6%) at 45 min after the second injection, provided that the second injection occurred 50 min after the first. In comparison rCMRglc1 reaches its minimum overall CV of 4.5% at 65 min after the first injection (Fig. 7).

Although, by giving the second FDG injection, the error in $\overline{C}\overset{*}{s}(T_2:T_1)$ from the use of erroneous rate

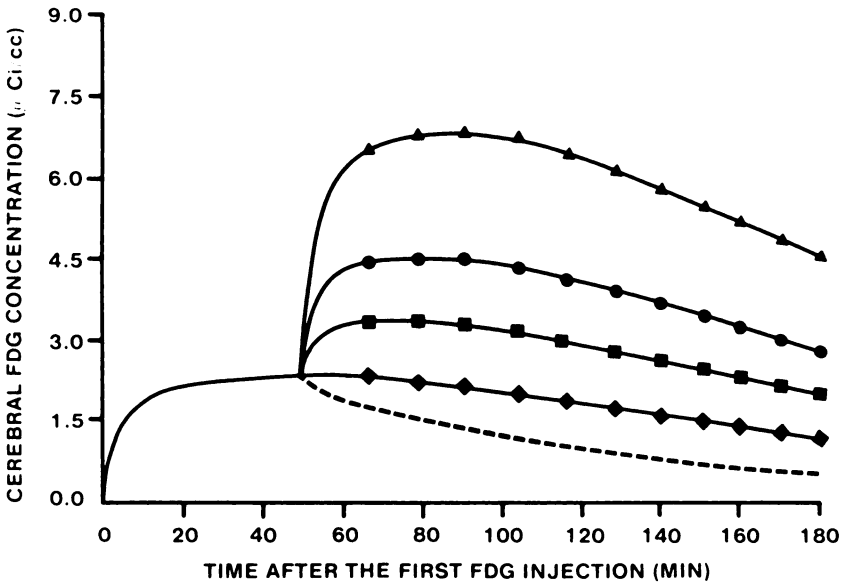

FIGURE 3
Time relationship between the simulated cerebral FDG concentration and the FDG injection dose ratios. The second FDG dose was injected at 50 min after the first FDG dose. The dashed line represents the theoretical tracer concentration reflecting the remnant of tracer after 50 min, assuming no further cerebral uptake from the remaining tracer in the plasma pool. Line with ◆, ■, ●, and ▲ represents an injection dose ratio of 1:0.0, 1:0.5, 1:1.0, and 1:2.0, respectively. The distance between the solid line and dash line is the magnitude of $C\hat{s}(T_2:T_1)$.

constant values is reduced (Fig. 4B–D), it does not reduce the error of rCMRglc2 to a proportional extent; the minimum error remains at the 5% level at injection-dose ratios of 1:0.5 to 1:2.0 (Fig. 8). Again, this occurs, because of cancellation of errors in $\bar{G}(T_2:T_1)$ and $\bar{C}\hat{s}(T_2:T_1)$, arising from use of erroneous values of k_2^* and k_3^*, but summation of errors from the use of an erroneous k_4^* value. The balance between the cancellation and summation of errors gives the same minimum error for different injection dose ratios, but the times at which minimum error of rCMRglc2 occur, vary. For ratios of 1:0.5, 1:1, and 1:2, the minimum error occurs at 35, 45, and 55 min, respectively.

Sensitivity of rCMRglc2 to Positioning Error

Figure 9 illustrates the manner in which measured values of tracer concentration change at different distances from a site at which a 25% step change in tracer concentration has occurred. Table 2 lists the value of percent errors added to CMRglc2 when the degrees of misalignment are 1, 2, 3, and 4 mm for PET devices with resolutions of 6, 9, and 15 mm (FWHM), respectively. These errors become smaller when the concentration change is not so steep (Table 2). Also, the magnitude of this error is dependent on the proportion of $R^*(T_2:T_1)$ to $C^*(T_2)$. Therefore, higher injection dose ratios, such as a 1:2 ratio will decrease the error in rCMRglc2 measurement by 1.7 times, compared to a 1:1 injection-dose ratio.

TABLE 1
Ratio of $Cs^*(T_2:T_1)$ to $R^*(T_2:T_1)$

	Time after the second FDG injection (min)*				
Injection-dose ratio	10	20	30	40	50
1.0 : 0.0	0.26	0.38	0.41	0.57	0.62
1.0 : 0.5	0.79	1.03	1.16	1.39	1.50
1.0 : 1.0	1.32	1.71	1.88	2.28	2.46
1.0 : 2.0	2.32	3.00	3.31	3.96	4.27

*Second FDG dose is injected at 50 min after the first FDG dose was injected.

Error of rCMRglc Estimation Arising from an Ill-Defined Scanning Period

Table 3 lists the percentage error in tracer concentration that results from discontinuing a behavioral task during the PET scanning period. These errors were calculated using different sets of rate constants to reflect a 20% higher metabolic rate during the 30-min period of activation, in comparison to the subsequent scanning period. From Table 3, it can be seen that the metabolic rate during the activation period is likely to be underestimated by 4% because of admixture of the activation period metabolic rate by the scanning period metabolic rate. For a true 20% increase of metabolism over the baseline, the measured increase will be 16%. This error is reduced when the scanning time is shortened from 20 min, used in these situations, to 10 min (error decreases from 2–5% to 1–3%). Such a reduction in scanning time may be feasible with high-sensitivity PET cameras.

DISCUSSION

The majority of PET studies on different disease conditions and physiological states are conducted using the isotope ^{18}FDG, because of the convenience in the use of this isotope, and because the measurement of glucose metabolism provides a sensitive index of brain dysfunction and physiological activation. The development of a procedure that allows two physiological states

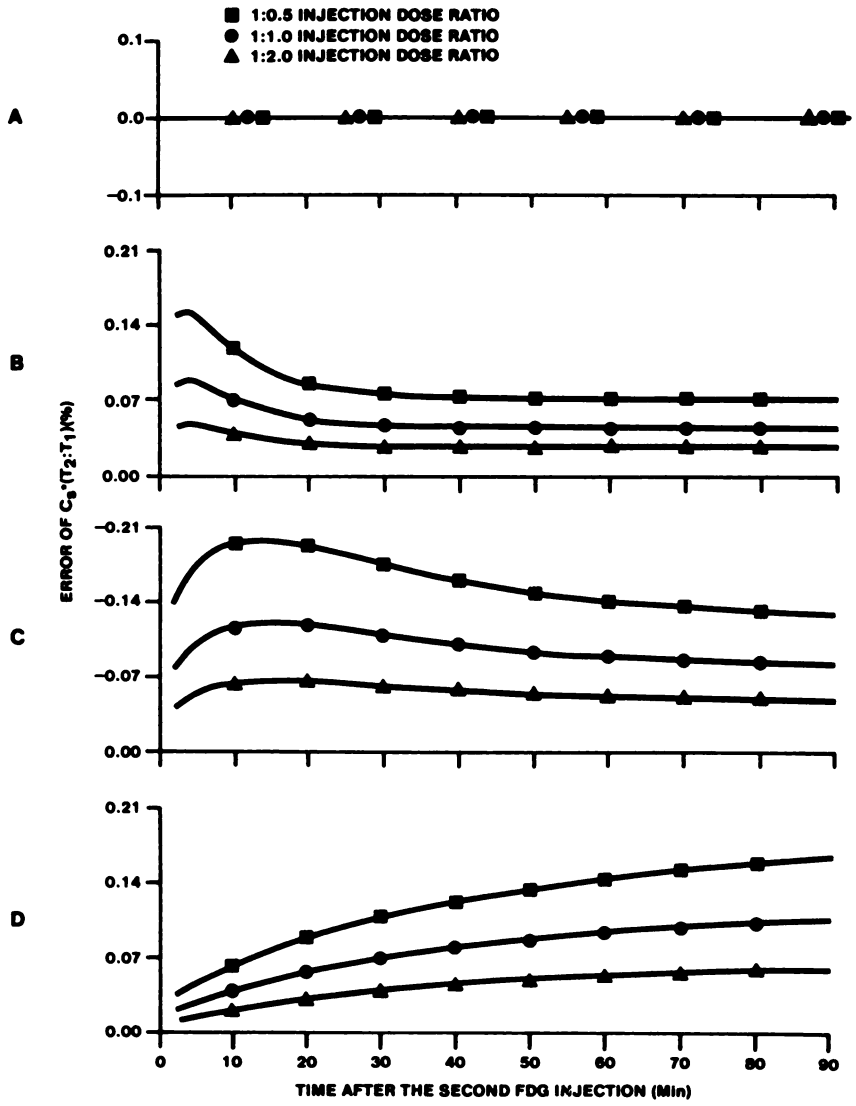

FIGURE 4
Error (%) of $\bar{C}s^*(T_2:T_1)$ from 1% error of k_1 (Fig. 4A), of k_2 (Fig. 4B), of k_3 (Fig. 4C), and of k_4 (Fig. 4D) for three different injection dose ratios.

to be studied in succession over a 100-min period using ^{18}FDG and PET (*1*), has been shown in our hands to be a valuable addition (*9–11*) to the original single injection method (*8*). However, the additional errors associated with measurement of rCMRglc in this fashion need to be recognized and quantified, as these will have a bearing on the ultimate utility of the procedure.

The errors associated with the use of average rate

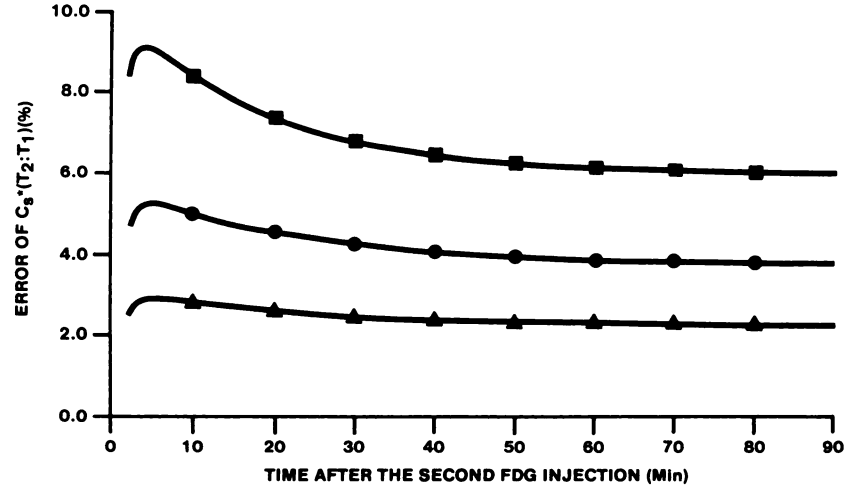

FIGURE 5
Expected error range (%) of $\bar{C}s^*(T_2:T_1)$, arising from the use of erroneous rate constant values, for three different injection dose ratios. Standard deviation of rate constants (published values) are used as the values of normal variation. Line with ■, ●, and ▲ represents an injection dose ratio of 1:0.5, 1:1.0, and 1:2.0, respectively.

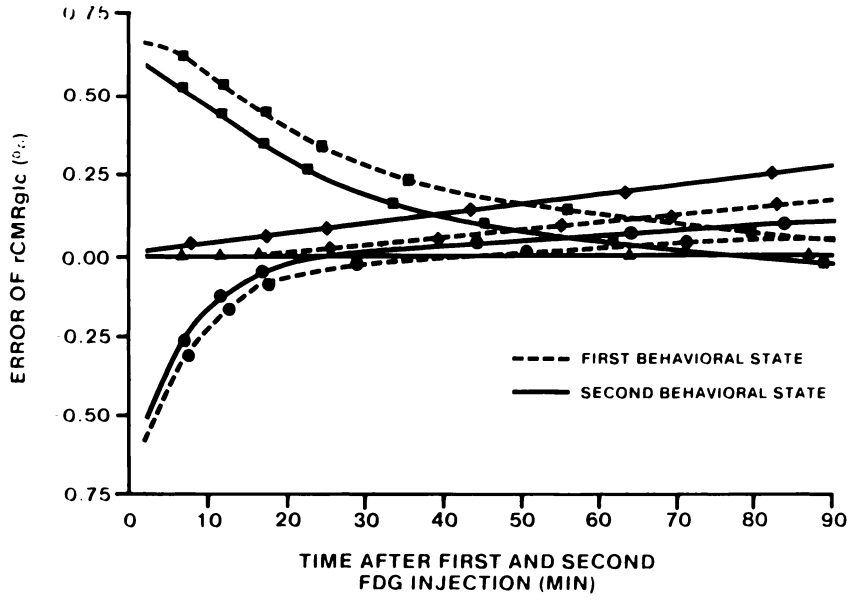

FIGURE 6
Error (%) of rCMRglc from 1% error in each respective rate constant value for the first and second behavioral states. Lines with ▲, ●, ■, and ◆ represents error from k_1^*, k_2^*, k_3^*, and k_4^*, respectively. The plots are obtained by using a 1:1 injection dose ratio.

constant values in the operational equation used to obtain rCMRglc have been examined (*2–4,6,7*), and these same errors apply to this double injection/double activation procedure, for rCMRglc1 estimation. We have addressed here the additional errors associated with rCMRglc2 estimation, using this double injection/double activation procedure. Although rate constant values vary greatly from subject to subject and region to region in normals (*2,12*), our results suggest the CV of $\overline{C}^*_s(T_2:T_1)$ using a 1:1 injection dose ratio is only 4.0%. This small error rate can be achieved partly because of radioactive decay of the isotope that remains in the brain from the first ^{18}FDG injection, and partly because error of $\overline{R}^*(T_2:T_1)$ is not sensitive to errors in rate constants. The results of our error analyses suggest that rCMRglc for both physiological states can be obtained with relatively low overall error (5% CV, excluding the statistical error that results from having a finite number of counts in each PET image), using average rate constant values.

A recent study (*12*) reported on regional rate constant values in normal volunteers, but limited measurements to k_1^*, k_2^*, and k_3^* only. The mean values of these recent measurements are in good agreement with the old values that were used here. But the variability about the mean for each new rate constant value is smaller than for the old values. Thus, using larger variance values for error analysis as we did here, we could have overestimated the overall error of rCMRglc. In addition, the much smaller variation of k_2^* reported in this recent study, i.e., 15% versus 50.8% used here, could result in the optimal time for starting the PET scan to be earlier. However, without an accurate knowledge of k_4^* and its variability, it is impossible to fully address the question of optimal time for starting the PET scan. To estimate the overall CV of rCMRglc from using

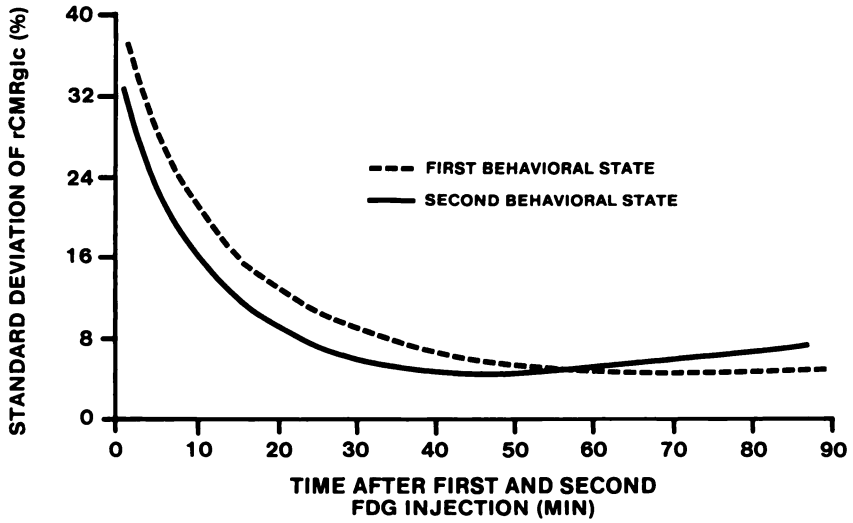

FIGURE 7
Expected error range (%) of rCMRglc, arising from the use of erroneous rate constant values, for first and second behavioral states. Standard deviation of rate constants (published values) are used as the values of normal variation. The plots were obtained from using 1:1 injection dose ratio and the second FDG dose was injected at 50 min after the first FDG dose.

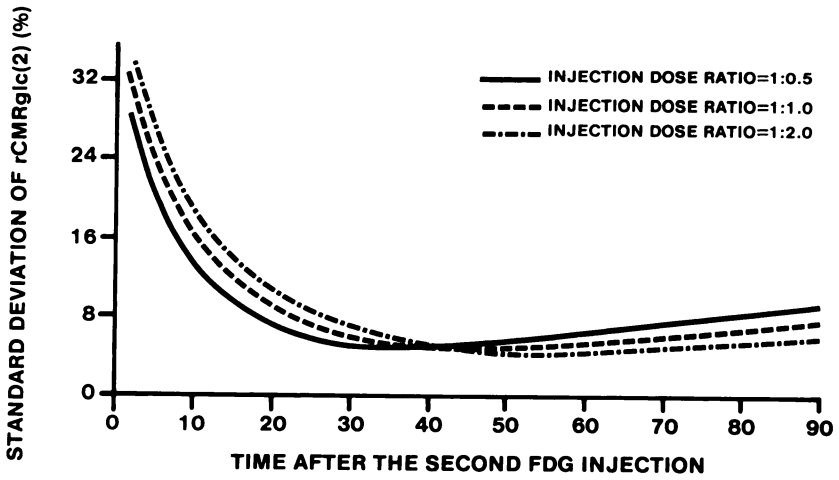

FIGURE 8
Expected error range (%) of rCMRglc2, arising from the use of erroneous rate constant values, for three different doses of second FDG injection. Standard deviation of rate constants (published values) are used as the values of normal variation.

average rate constant values, we have assumed the values of each rate constant are not correlated with one another. However, it has been shown that k_1^* and k_2^* are fairly closely correlated with each other, but there is no significant correlation among the other rate constants (*12*). Therefore, the calculation of overall error should consider the covariance of k_1^* and k_2^*. Nevertheless, the error of rCMRglc is insensitive to errors of k_1^* and, so also its product with the error of k_2^*. Thus, the calculation of overall error is not generally affected by the correlation of the values of the rate constants k_1^* and k_2^*.

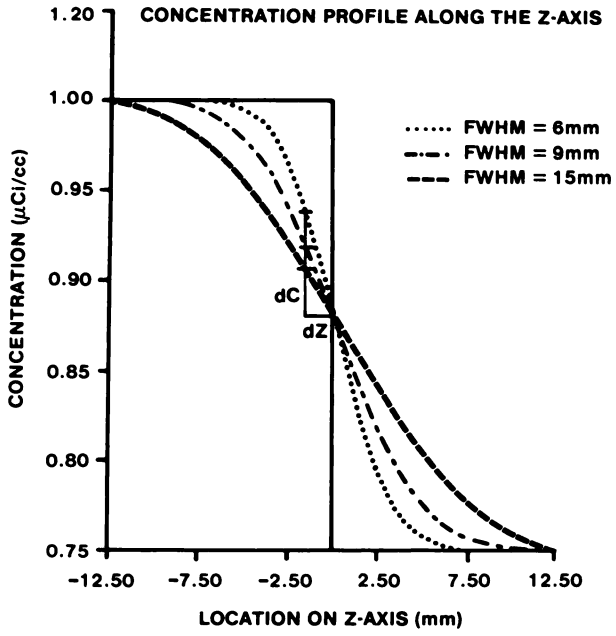

FIGURE 9
Simulated concentration profiles along the z-axis measured by PET device with different resolution along the z-axis. The solid line represents the true concentration profile along the z-axis.

Statistical error from PET measurement related only to using the PET device to measure ^{18}F concentration in tissue is additional to the error of rCMRglc measurement that we have mentioned. Its magnitude depends on how this statistical error is propagated from measurement of tracer concentration in tissue to metabolic rate values. For rCMRglc1, this error is propagated linearly, i.e., percent error in measurement of $C^*(T_1)$ can be added directly to other errors in estimation of rCMRglc1. For rCMRglc2, this statistical error is also propagated linearly, but is more complex because it involves subtraction of a fraction of $C^*(T_1)$ from $C^*(T_2)$, which is related to time between T_1 and T_2 (Appendix 2). It is clear that the statistical noise associated with rCMRglc1 and rCMRglc2 estimations can be of unequal magnitude if the injection dose ratio and/or scan times are different. Thus, by appropriate adjustment of the length of the scanning period and behavioral state, and the dose of the second FDG injection, equivalent and minimal statistical noise levels for each rCMRglc measurement can be achieved.

In Figure 8, it can be seen that the minimum error of rCMRglc2, arising from the use of erroneous values of rate constants, is not affected by the second FDG injection dose. However, the statistical noise in rCMRglc2 measurement is affected by the second FDG injection dose. Table 4 shows how the statistical error is reduced by changing the injection dose ratio. For a 1:0.5 ratio, rCMRglc2 will have a statistical noise ~1.51 times larger than the statistical noise of rCMRglc1, provided both scanning periods (data collection times) are of equal length. A longer second PET scanning period to compensate for the small second injection dose will improve the statistical noise in rCMRglc2 measurement, but at the expense of dilution of the specific activation condition with a nonspecific condition. A large second FDG injection dose will also reduce statistical noise in rCMRglc2 but at the expense of

TABLE 2
Error (%) of CMRglc2 Arising from Slice Misalignment*

Concentration profile	FWHM (mm)†	Amount of misalignment 1 mm	2 mm	3 mm	4 mm
25% step change	6	7.1 (4.2)‡	13.1 (7.9)	17.5 (10.5)	20.2 (12.2)
	9	4.8 (2.9)	9.3 (5.6)	13.3 (8.0)	16.5 (9.9)
	15	3.1 (1.9)	6.1 (3.7)	9.0 (5.4)	11.7 (7.0)
25% change over a 5-mm distance	6	6.3 (3.8)	11.9 (7.2)	16.5 (9.9)	19.7 (11.8)
	9	4.6 (2.8)	8.9 (5.4)	12.8 (7.7)	16.0 (9.6)
	15	3.0 (1.8)	6.0 (3.6)	8.9 (5.3)	11.5 (6.9)
25% change over a 10-mm distance	6	4.5 (2.7)	8.8 (5.3)	12.8 (7.7)	16.2 (9.7)
	9	3.8 (2.3)	7.5 (4.5)	10.9 (6.6)	14.0 (8.4)
	15	2.8 (1.7)	5.6 (3.4)	8.3 (5.0)	10.8 (6.5)

* The estimated error is obtained from a 1:1 injection dose ratio, assuming there is a true 25% difference of tracer concentration at z=0mm and CMRglc1=CMRglc2.
† FWHM of the point spread function along the z-axis.
‡ The numbers outside of the parenthesis come from the double injection/double activation method; the numbers inside of the parenthesis come from two independent FDG/PET studies.

increasing the radiation dose delivered to the subject. An injection dose ratio of 1:1 is perhaps the best compromise, giving equivalent statistical noise levels for both scans, and allowing equivalent scanning periods, with what we consider acceptable radiation dose to the subject.

The error sensitivities of rCMRglc to each rate constant behave differently with respect to time after each FDG injection. As can be seen in Figure 7, it may be advantageous to allow the first period of tracer uptake and scanning to last for 70 min, instead of 50 min, so that error of rCMRglc1 estimation decreases to a minimum. Since such a modification would entail delaying the second injection, we have compared the error of $\overline{Cs}^*(T_2:T_1)$, due to a 1% error in rate constant values, when the second injection is at 70 min versus at 50 min (Fig. 10). The plots demonstrate that the error sensitivity of $\overline{Cs}^*(T_2:T_1)$ to rate constants have the same characteristics for the two second injection times, but the magnitudes are slightly different. The error sensitivities of $\overline{Cs}^*(T_2:T_1)$ to error in k_2^* and k_3^* decrease as the second FDG dose is injected later, whereas the error sensitivity of $\overline{Cs}^*(T_2:T_1)$ to k_4^* simultaneously increases. As a result, the CV of $\overline{Cs}^*(T_2:T_1)$ reaches a minimum at 35 min after the second injection, when this is given at 70 min. This minimum is reached 30 min earlier than when the second dose of FDG is injected at 50 min (Fig. 11). Thus, the best time (time with the least rCMRglc error arising from using erroneous rate con-

TABLE 3
Percent Underestimation of Brain Tracer Concentration When the Behavioral Task is Not Continued During the Scanning Period

Set no.†	Scan time 20 min	10 min	5 min
1	4.6	2.7	1.7
2	5.5	3.2	2.0
3	2.1	0.9	0.6
4	3.8	2.1	1.6
5	4.4	2.6	1.6
6	5.4	3.1	1.9
7	3.5	0.9	0.6
8	3.9	2.1	1.3
9	4.8	2.9	1.9
10	5.7	3.4	2.2
11	2.1	0.9	0.6
12	3.8	2.2	1.4
Mean	4.1	2.3	1.5

* The results were obtained using the same duration for each behavioral state (i.e., 50 min).
† Set # refers to Appendix 2.

TABLE 4
Ratio of Percent Error of $C^*(T_2)$ to $C^*(T_1)$ and $\overline{Cs}^*(T_2:T_1)$ to $C^*(T_1)$*

Injection dose ratio	$\left(\frac{\Delta C^*(T_2)}{C^*(T_2)}\right) / \left(\frac{\Delta C^*(T_1)}{C^*(T_1)}\right)$	$\left(\frac{\Delta \overline{Cs}^*(T_2:T_1)}{\overline{Cs}^*(T_2:T_1)}\right) / \left(\frac{\Delta C^*(T_1)}{C^*(T_1)}\right)$
1:0.0	1.08	2.93
1:0.5	0.87	1.51
1:1.0	0.73	1.07
1:2.0	0.59	0.77

* The error is due to Poisson fluctuation in the projection data.

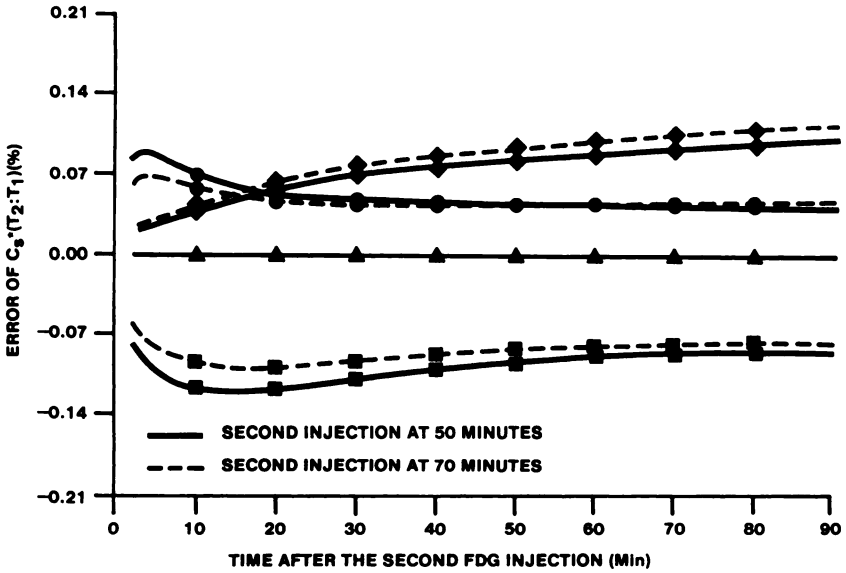

FIGURE 10
Error (%) of $\overline{Cs}^*(T_2:T_1)$ from 1% error in each respective rate constant value for two different injection time sequences. Lines with ▲, ■, ●, and ◆ represents error from k_1^*, k_2^*, k_3^*, and k_4^*, respectively. The plots are obtained by using a 1:1 injection dose ratio.

stant values) for PET scanning occurs at 50 min after the first FDG injection, but at 20 min after the second FDG injection (assuming a 20-min scanning period), provided the second injection is at 70 min after the first injection and the injection dose ratio is 1:1. Thus, to minimize errors arising from the use of erroneous rate constants, the duration of the behavioral states would have to be unequal, i.e., 70 min and 40 min. However, it is inadvisable to allow the two behavioral states to be of unequal duration because it may compromise various physiological or psychological paradigms. Other considerations such as fatigue, habituation, and physical discomfort of the subject, and the advantage of having a short behavioral state also come into play.

We have adopted the procedure of using a 1:1 injection dose ratio and equal scan time, as this allows equal statistical noise for the two rCMRglc measurements (Table 4) and equal duration for each behavioral state. Fifty minutes was chosen to be the length of each behavioral state (including 20-min scanning period) so that the error of rCMRglc2 would remain minimal, even though the CV of rCMRglc1 would increase from 4.2% to 5.2%.

The method by which $\overline{Cs}^*(T_2:T_1)$ is estimated is based on the measured tracer concentration in the second scan, $C^*(T_2)$, and the estimated amount of residual tracer from the first state. If there is a substantial change of metabolic rate between the first and second state, because of an alteration in e.g., the behavioral state or the use of a pharmacologic agent, this would potentially have an impact on the accuracy of $\overline{Cs}^*(T_2:T_1)$ measurement. For a 20% metabolic rate increase, the CV of $\overline{Cs}^*(T_2:T_1)$ is ~3.5%; whereas for a 20% decrease in metabolic rate, the CV of $\overline{Cs}^*(T_2:T_1)$ is ~4.5%. Therefore, using a 1:1 injection dose ratio, an alteration of metabolic rate of 20% between the first and second state, results in an additional 0.5% error to $\overline{Cs}^*(T_2:T_1)$

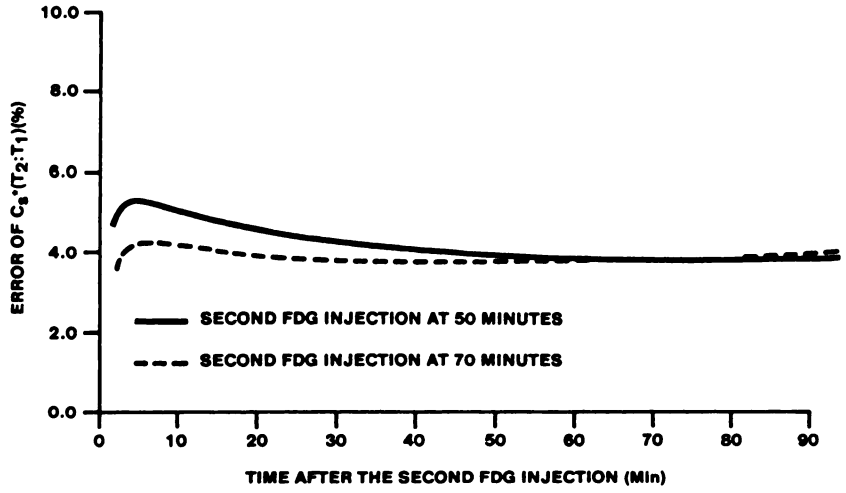

FIGURE 11
Expected error range (%) of $\overline{Cs}^*(T_2:T_1)$, arising from the use of erroneous rate constant values, for two different times at which the second FDG injection was made. Standard deviation of rate constants (published values) are used as the values of normal variation.

estimation (from the minimum of 4.0%) and rCMRglc2, as well.

As may be expected from the rapid reduction in the plasma levels of tracer after the time of injection, alterations of rCMRglc that occur because of behavioral or other distortions at time periods >30 min after injection have very little impact on the measured metabolic rate for the first 30-min period. Thus our data shows that the nonspecific behavioral state during scanning, that follows the specific behavioral state in the first 30 min, has only a minor effect on calculated rCMRglc values.

Exact repositioning of the patient is of great importance in this procedure and, if achieved, allows a single set of regions of interest (ROIs) to be defined and used for both scans. However, possibly because of movement of the patient during the scanning period and/or repositioning error for the second scan, exact repositioning may not be achieved. Consequently, certain error can be added to rCMRglc2 estimation. These errors, which are unique to this double-injection/double-activation procedure, are ~1.6-fold larger than the errors generated when the second PET/FDG studies is done at different times. The additional errors come from using erroneous values of $R^*(T_2:T_1)$ when the double activation/double injection method is used.

In a previous publication (*1*), we have examined the reproducibility of rCMRglc values, when the same behavioral task was repeated, using this double-injection strategy. Two behavioral tasks, namely the word fluency task (WFT) and picture preference task (PPT) were each used in a repeated fashion (WFT-WFT and PPT-PPT) and across brain regions the average CV for (rCMRglc2-rCMRglc1)/rCMRglc1 were 4.2% and 6.2%, respectively. The range of variability across different structures were 3.4% to 8.6% for PPT-PPT and 0.9% to 8.5% for WFT-WFT.

To compare these observed errors from WFT-WFT and PPT-PPT to the predicted error obtained from the results of our error analysis, we have considered: (a) the CV of (rCMRglc2-rCMRglc1)/rCMRglc1, arising from the use of erroneous values of rate constants (4.0%) (Appendix 4), (b) the root mean square of statistical error for percent difference obtained from subtraction of the two PET images (3%), (c) error in rCMRglc2 estimation arising from misalignment (averaged at 4%), (d) error arising from disruption of a specified behavioral steady-state by the nonspecific state of the scanning period (4%). The root mean square of the first three errors (6.4%) gives the total error that might be expected in the average double-injection study, when the same behavioral state is repeated. This total error, predicted theoretically, is in good agreement with the observed error from WFT-WFT (4.2%) and PPT-PPT (6.2%).

In summary, utilizing a double-injection procedure with an injection-dose ratio of 1:1 and 50 min for each period of tracer uptake and scanning, the total error predicted in terms of percent difference is 6.4%. Intrinsically the double-injection procedure adds 60% more error to rCMRglc estimation for the second scan than would be obtained in an independent second FDG/PET scan. However, it is clear from our previous studies (*13*) that intra-individual variability of rCMRglc is in the order of 25% when studies are done on different days, and is substantially lower (7%) (*14*) when done 2 hr apart, using [^{14}C]deoxyglucose. These differences in rCMRglc obtained on different days are likely to be largely related to true physiological variations that occur. It is likely that the double-injection method, which offers greater likelihood of accurate repositioning and a short interval between the two scans, will be more precise, and will be found to be more convenient than two separate FDG/PET scans done on different days.

APPENDIX 1

Summary of the Definition of the Terms

Terms	Definition
$C^*(T_1)$, $C^*(T_2)$	Tissue concentration of tracer at T_1 and T_2, respectively.
$T_2:T_1$	Described event happened after T_1 then continued to T_2
$R^*(T_2:T_1)$	The remnant of tracer concentration at T_1 that is present at T_2.
$\bar{R}^*(T_2:T_1)$	Estimated $R^*(T_2:T_1)$ using average rate constant values.
$Cs^*(T_2:T_1)$	Tracer concentration at T_2 as the result of tracer uptake from T_1 to T_2 during the second state.
$\bar{C}s^*(T_2:T_1)$	Estimated $Cs^*(T_2:T_1)$ using average rate constant values.
Ce^*,Cm^*	Tissue concentration of free FDG and FDG-6-P, respectively.
$\bar{C}e^*$, $\bar{C}m^*$	Estimated Ce^* and Cm^* using average rate constant values
CV	Coefficient of variation

APPENDIX 2

The relationship between $\bar{C}s^*(T_2:T_1, Z_0)$, $C^*(T_1, Z_0)$, and $C^*(T_2, Z_0)$ are expressed as follows:

$$\bar{C}s^*(T_2:T_1, Z_0) = C^*(T_2, Z_0) - C^*(T_1, Z_0)Q \qquad (A1)$$

where

$$Q = \bar{B}(T_2:T_1) - \bar{A}(T_2:T_1)$$

since both $C^*(T_2)$ and $C^*(T_1)$ are independent variables, the variance of $\bar{C}s^*(T_2:T_1)$ can be expressed as follows:

$$\text{var}(\bar{C}s^*(T_2:T_1)) = \text{var}(C^*(T_2)) + \text{var}(C^*(T_1))Q^2.$$

Repositional Error

The error of $\bar{C}^*_s(T_2{:}T_1, Z_0)$ estimation results from misalignment is due to the repositional error of $C^*(T_2, Z_0)$ relative to $C^*(T_1, Z_0)$, thus the variance of $C^*(T_1, Z_0)$ is equal to zero and

$$\frac{\mathrm{var}(\bar{C}^*_s(T_2{:}T_1, Z_0))}{\bar{C}^*_s(T_2{:}T_1, Z_0)^2} = \frac{\mathrm{var}(C^*(T_2, Z_0))}{C^*(T_2, Z_0)^2}\frac{C^*(T_2, Z_0)^2}{\bar{C}^*_s(T_2{:}T_1, Z_0)^2}, \quad \text{(A2)}$$

since $\bar{C}^*_s(T_2{:}T_1, Z_0)$ is equal to $C^*(T_2, Z_0) - \bar{R}^*(T_2{:}T_1, Z_0)$.

The relationship of percent error of $\bar{C}^*_s(T_2{:}T_1, Z_0)$ and $\bar{R}^*(T_2{:}T_1, Z_0)$, resulting from repositional error, can be rearranged as:

$$\frac{\Delta\bar{C}^*_s(T_2{:}T_1, Z_0)}{\bar{C}^*_s(T_2{:}T_1, Z_0)} \times 100\% = \frac{\dfrac{\Delta C^*(T_2, Z_0)}{C^*(T_2, Z_0)}}{1 - \dfrac{R^*(T_2{:}T_1, Z_0)}{C^*(T_2, Z_0)}} \times 100\%$$

Z_0 is the location along the z-axis.

Statistical Error

The statistical error of both $C^*(T_1, Z_0)$ and $C^*(T_2, Z_0)$ obtained from using PET are contributing to the final error of $\bar{C}^*_s(T_2{:}T_1, Z_0)$. Thus, the percent error of $\bar{C}^*_s(T_2{:}T_1, Z_0)$ can be expressed as:

$$\frac{\mathrm{var}(\bar{C}^*_s(T_2{:}T_1))}{\bar{C}^*_s(T_2{:}T_1)^2} = \frac{\mathrm{var}(C^*(T_2))}{C^*(T_2)^2}\frac{C^*(T_2)^2}{\bar{C}^*_s(T_2{:}T_1)^2} + \frac{\mathrm{var}(C^*(T_1))}{C^*(T_1)^2}\frac{C^*(T_1)^2}{\bar{C}^*_s(T_2{:}T_1)^2}Q^2.$$

APPENDIX 3

Listed Below are the 12 Sets of Rate Constant Values Used in the Computer Program to Simulate a 20% Change of Metabolic Rate Between the Activated State and Resting State

Set no.*	FDG Transport Rate Constants of Various Simulated Metabolic Rates in Tissue: Activated state (CMR_1) k_1^*	k_2^*	k_3^*	k_4^*	$k_1^*k_3^*/(k_2^*+k_3^*)$
1	0.1224	0.1300	0.0620	0.0068	0.0395
2	0.1020	0.0980	0.0620	0.0068	0.0395
3	0.1020	0.1300	0.0823	0.0068	0.0395
4	0.1091	0.1214	0.0690	0.0068	0.0395
5	0.1346	0.1254	0.0682	0.0068	0.0474
6	0.1122	0.0931	0.0682	0.0068	0.0474
7	0.1122	0.1254	0.0918	0.0068	0.0474
8	0.1192	0.1138	0.0752	0.0068	0.0474
9	0.1102	0.1386	0.0558	0.0068	0.0316
10	0.0918	0.1062	0.0558	0.0068	0.0316
11	0.0918	0.1386	0.0728	0.0068	0.0316
12	0.0990	0.1321	0.0620	0.0068	0.0316

Set no.*	Resting state (CMR_2) k_1^*	k_2^*	k_3^*	k_4^*	$k_1^*k_3^*/(k_2^*+k_3^*)$	CMR_1/CMR_2†
1	0.1020	0.1300	0.0620	0.0068	0.0329	1.2
2	0.1020	0.1300	0.0620	0.0068	0.0329	1.2
3	0.1020	0.1300	0.0620	0.0068	0.0329	1.2
4	0.1020	0.1300	0.0620	0.0068	0.0329	1.2
5	0.1122	0.1254	0.0682	0.0068	0.0395	1.2
6	0.1122	0.1254	0.0682	0.0068	0.0395	1.2
7	0.1122	0.1254	0.0682	0.0068	0.0395	1.2
8	0.1122	0.1254	0.0682	0.0068	0.0395	1.2
9	0.0918	0.1386	0.0558	0.0068	0.0263	1.2
10	0.0918	0.1386	0.0558	0.0068	0.0263	1.2
11	0.0918	0.1386	0.0558	0.0068	0.0263	1.2
12	0.0918	0.1386	0.0558	0.0068	0.0263	1.2

* See text for description of this term.

† CMR_1 is the metabolic rate during the behaviorally activated state, CMR_2 is the metabolic rate during the scanning period.

APPENDIX 4

The percent difference of rCMRglc between the two states can be expressed as follows:

$$\Delta\% = \frac{\mathrm{rCMRglc2} - \mathrm{rCMRglc1}}{\mathrm{rCMRglc1}} = \frac{\dfrac{Cp\,\bar{k}_1^*\bar{k}_3^*}{LC\,\bar{k}_2^* + \bar{k}_3^*}\left[\dfrac{\bar{C}^*_s(T_2{:}T_1)}{\bar{C}^*_e(T_2{:}T_1)+\bar{C}^*_m(T_2{:}T_1)} - \dfrac{C^*(T_1)}{\bar{C}^*_e(T_1)+\bar{C}^*_m(T_2)}\right]}{\dfrac{Cp\,\bar{k}_1^*\bar{k}_3^*}{LC\,\bar{k}_2^* + \bar{k}_3^*}\dfrac{C^*(T_1)}{[\bar{C}^*_e(T_1)+Cm(\bar{T}_1^*)]}}$$

$$= \frac{\dfrac{\bar{C}^*_s(T_2{:}T_1)}{C^*(T_1}}{\dfrac{[\bar{C}^*_e(T_2{:}T_1) + \bar{C}^*_m(T_2{:}T_1)]}{[\bar{C}^*_e(T_1) + \bar{C}^*_m(T_2)]}} - 1.$$

Since the blood curves from both studies are very similar, the denominator becomes a constant and is not sensitive to the change of rate constant values. As a result, the error sensitivity of percent difference to error of rate constant values is directly related to error of $\bar{C}^*_s(T_2{:}T_1)$.

ACKNOWLEDGMENT

Preliminary reports of this work were made at the 34th Annual Meeting of the Society of Nuclear Medicine, Toronto, June 2–5, 1987 and 13th International symposium on Cerebral Blood Flow and Metabolism, Montreal, June 20–25, 1987.

This project is funded partially under an agreement with the Aging and Adult Services Program Office, Department of Health and Rehabilitative Services, State of Florida (Contract MG 805). Also supported by USPHS grants NS21720, NS05820, and NS22603. Other support is from general research funds from Mount Sinai Medical Center, Miami Beach, Florida.

REFERENCES

1. Chang JY, Duara R, Barker W, Apicella A, Finn R. Two behavioral state studied in a single PET/FDG procedure: theory, method, and preliminary results. *J Nucl Med* 1987; 28:852–860.
2. Huang SC, Phelps ME, Hoffman EJ, et al. Noninvasive determination of local cerebral metabolic rate of glucose in man. *Am J Physiol* 1980; 238:E69–E82.
3. Brooks RA. Alternative formula for glucose utilization using labeled deoxyglucose. *J Nucl Med* 1982; 23:538.
4. Hutchins GD, Holden JE, Koeppe RA, et al. Alternative approach to single-scan estimation of cerebral glucose metabolic rate using glucose analogs with particular application to ischemia. *J Cereb Blood Flow Metab* 1984; 4:35–40.
5. Kearfott K, Rottenberg D, Knowles R, et al. A new headhold for PET, CT, and NMR imaging. *J Comput Assist Tomogr* 1984; 8:1217–1220.
6. Huang S, Phelp M, Hoffman E, et al. Error sensitivity of fluorodeoxyglucose method for measurement of cerebral metabolic rate of glucose. *J Cereb Blood Flow Metab* 1981; 1:391–401.
7. Kato A, Menon D, Diksic M, et al. Influence of the input function on the calculation of the local cerebral metabolic rate for glucose in the deoxyglucose method. *J Cereb Blood Flow Metab* 1984; 4:41–46.
8. Sokoloff L, Reivich M, Kennedy C, et al. The [^{14}C] deoxyglucose method for the measurement of local cerebral glucose utilization: theory, procedure and normal values in the conscious and anesthetized albino rate. *J Neurochem* 1977; 28:897–916.
9. Ginsberg MD, Yoshii F, Vibulsresth S, et al. Human task-specific somatosensory activation. *Neurology* 1987; 37:1301–1308.
10. Ginsberg MD, Chang JY, Kelley RE, et al. Increases in both cerebral glucose utilization and blood flow during execution of a somatosensory task. *Ann Neurol* 1988; 23:152–160.
11. Duara R, Yoshii F, Chang J, et al. Complex reading memory task during PET in normal and memory-impaired subjects. *J Cereb Blood Flow Metab* 1987; 7(suppl):S312.
12. Heiss W, Pawlik G, Herholz R, et al. Regional kinetic constant and cerebral metabolic rate for glucose in normal human volunteers determined by dynamic positron emission tomography of [^{18}F]-2-fluoro-2-deoxy-D-glucose. *J Cereb Blood Flow Metab* 1984; 4:212–233.
13. Duara R, Gross-Glenn K, Barker WW, et al. Behavioral activation and the variability of cerebral glucose metabolic measurements. *J Cereb Blood Flow Metab* 1987; 7:266–271.
14. Reivich M, Alavi A, Wolf A, et al. Use of 2-deoxy-D-(1-^{11}C) glucose for the determination of local cerebral glucose metabolism in humans: variation within and between subjects. *J Cereb Blood Flow Metab* 1982; 2:307–319.